A Review of Sodium Oxalate Solubility in Water

Jacob G. Reynolds,* Michael D. Britton, and Robert Carter

Cite This: *Ind. Eng. Chem. Res.* 2023, 62, 19394−19401

Read Online

ACCESS | Metrics & More | Article Recommendations

ABSTRACT: The solubility of disodium oxalate is important to many industries. This study compiled and statistically assessed the disodium oxalate solubility data available between 273 and 373 K. Sixty-six measurements were found from 19 studies. Two additional studies published their data graphically. The solubility was found to be an approximately linear function of the temperature, increasing about 0.0027 mol/kg per K. The coefficient of determination (R^2) of a linear fit to the data was 0.98. The mean measured solubility at 298.15 K was 0.274 mol/kg, with a standard error of 0.0026, with good agreement across data sets. The data were compared to calculated solubilities using a previously published thermodynamic model and shown to have reasonable agreement. The solubility of disodium oxalate was less than other alkali oxalates. Oxalate has a −2 charge, or −0.5 charge per oxygen, and an average bond valence of −0.17 per coordinating cation. Disodium oxalate is less soluble than other alkali oxalates because Na$^+$ has a more closely matching opposite bond valence (0.16) than do other alkali cations. This is consistent with Brown's theory that the most stable solids are those where cation and anions have matching opposite bond valence without having to adjust to uncommon bond lengths or coordination numbers.
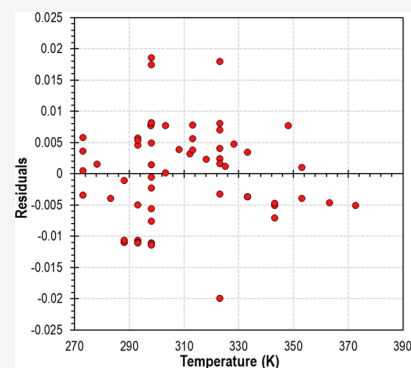
INTRODUCTION

Disodium oxalate (Na$_2$C$_2$O$_4$; CAS 62-76-0) is important to many chemical industries. Oxalate is used industrially for rare earth and actinide processing.[1−6] The solubility of disodium oxalate is thus required to develop flowsheets for those processes. In nature, disodium oxalate is called natroxalate, and its solubility can influence the fate of oxalate in sedimentary environments.[7,8]

Many large organics degrade into oxalates in high pH aqueous solutions. Consequently, industries with organics in high pH solutions often have oxalate as an impurity. These industries include pulp and paper as well as the Bayer alumina refining process. Disodium oxalate can be at high enough concentration in those processes to cause process upsets.[9−13]

The solubility of disodium oxalate is not only of interest to industries that use it but is also an input to alternative analyses for reagent selection. For instance, recent hydrometallurgical process development teams chose to use dipotassium oxalate as a reagent instead of disodium oxalate because of the higher solubility of dipotassium oxalate.[14,15]

The impetus for the present study is to better understand oxalate behavior in alkaline nuclear waste at sites such as Hanford and Savannah River in the United States. The Hanford Site maintains an inventory of nuclear waste constituents in a database called the Tank Waste Inventory Network System. That database indicates that there is about 1.4 million kilograms of oxalate in the waste tanks at Hanford. This equates to 16 million moles of oxalate. Oxalate is found in these wastes in both the liquid and as solid disodium

oxalate.[16−18] Oxalate was generated as a reaction product of a nitric acid destruction process using sugar.[20] Oxalate was also generated from the degradation of larger organics in the waste.[21−25] Oxalic acid was used to clean out nearly empty tanks in the past, where the subsequent neutralization created disodium oxalate.[26,27] Given that oxalate occurs in both the solid and liquid phases in nuclear waste, the solubility of disodium oxalate is of interest.[28]

The Hanford Site has developed models of the solubility of disodium oxalate and other salts.[29−32] The present authors are collecting and assessing the literature data to support model updates. The only common reference book we found containing the solubility of disodium oxalate in water over a large temperature range was the 1985 edition of Lange's Handbook of Chemistry, but that data was removed by the 1999 edition.[33,34] We are therefore sharing our review of the literature data on disodium oxalate solubility with the scientific community here. The data are compiled and statistically assessed. This study compliments existing reviews of the dissociation constants of oxalic acid as well as reviews of the solubility of other salts relevant to Hanford waste.[35−39] This study also compliments a recent study on the solubility trends
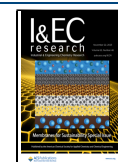
Table 1. Measurements of the Solubility of Disodium Oxalate in Water

ref	temp (K)	$Na_2C_2O_4$ solubility	original units	solubility (mol/kg)	ref	temp (K)	$Na_2C_2O_4$ solubility	original units	solubility (mol/kg)
42	273.15	2.62	wt %	0.201	57	298.15	3.73	wt %	0.289
43	273.15	2.71	wt %	0.208	44	303.15	0.284	mol salt/kg water	0.284
44	273.15	0.210	mol salt/kg water	0.210	45	303.15	3.76	wt %	0.292
45	273.15	2.67	wt %	0.205	44	308.15	0.301	mol salt/kg water	0.301
44	278.15	0.219	mol salt/kg water	0.219	58	312.15	4.0	wt %	0.311
45	283.15	2.95	wt %	0.227	42	313.15	4.09	wt %	0.318
47	288.15	3.1266	g/100 g water	0.233	44	313.15	0.316	mol salt/kg water	0.316
47	288.15	3.1226	g/100 g water	0.233	44	313.15	4.04	wt %	0.314
47	288.15	3.1234	g/100 g water	0.233	44	318.15	0.326	mol salt/kg water	0.326
47	288.15	3.1271	g/100 g water	0.233	59	323.15	4.28	wt %	0.334
44	288.15	0.243	mol salt/kg water	0.243	42	323.15	4.37	wt %	0.341
48	291.15	0.2400	mol/L	0.242*	54	323.15	0.317	mol salt/kg water	0.317
47	293.15	3.3058	g/100 g water	0.247	54	323.15	0.344	mol salt/kg water	0.344
47	293.15	3.3009	g/100 g water	0.246	60	323.15	4.35	wt %	0.339
47	293.15	3.3000	g/100 g water	0.246	44	323.15	0.345	mol salt/kg water	0.345
44	293.15	0.263	mol salt/kg water	0.263	45	323.15	4.34	wt %	0.339
45	293.15	3.39	wt %	0.262	57	323.15	4.54	wt %	0.355
46	293.15	3.40	wt %	0.263	58	325.15	4.4	wt %	0.343
49	293.15	3.27	wt %	0.252	44	328.15	0.355	mol salt/kg water	0.355
50	297.86	0.005	mol/mol water	0.278	43	333.15	4.60	wt %	0.360
51	298.15	0.2676	mol/L	0.270[a]	43	333.15	4.60	wt %	0.360
47	298.15	3.4779	g/100 g water	0.260	44	333.15	0.367	mol salt/kg water	0.367
47	298.15	3.4758	g/100 g water	0.259	45	333.15	4.60	wt %	0.360
47	298.15	3.4725	g/100 g water	0.259	54	343.15	0.385	mol salt/kg water	0.385
52	298.15	3.6	wt %	0.279[b]	54	343.15	0.383	mol salt/kg water	0.383
53	298.15	3.6	wt %	0.279[b]	45	343.15	4.91	wt %	0.385
42	298.15	3.56	wt %	0.275	60	348.15	5.22	wt %	0.411
54	298.15	0.272	mol salt/kg water	0.272	43	353.15	5.30	wt %	0.418
54	298.15	0.265	mol salt/kg water	0.265	45	353.15	5.24	wt %	0.413
54	298.15	0.263	mol salt/kg water	0.263	45	363.15	5.55	wt %	0.439
43	298.15	3.60	wt %	0.279	45	372.78	5.85	wt %	0.464
43	298.15	3.60	wt %	0.279					
55	298.15	3.47	wt %	0.268					
56	298.15	0.278	mol/L	0.281[a]					
44	298.15	0.270	mol salt/kg water	0.270					

[a]Calculated using water contents determined from the Laliberte-Cooper Model (see text). [b]These are a single measurement reported in two separate publications and should not be taken as two unique measurements.

of salts in multicomponent solutions simulating nuclear waste.[40]

The Hanford Site has been using a solubility model based on Pitzer's equations for liquid phase activities (eqs 1 and 2).[41] In those equations, m is the molality of ion, γ_i is the activity coefficient, γ_i^{DH} is the modified form of the Debye–Huckel activity coefficient, I is ionic strength, B_0 and B_1 are binary Pitzer parameters for each pair of ions, and C_{ijk} is another binary Pitzer parameter that is usually taken to be independent of ionic strength. The α parameter is a universal constant.[41]

$$\ln \gamma_i = \ln \gamma_i^{DH} + \sum B_{ij}(I)m_j + \sum_j \sum_k C_{ijk}m_j m_k + \cdots \quad (1)$$

$$B_{ij} = B_0 + B_1 \exp(-\alpha I^{0.5}) \quad (2)$$

◼ DATA REVIEW

Given the industrial interest in disodium oxalate solubility, many researchers have studied oxalate solubility between 273 and 373.15 K (Table 1). Table 1 contains the data found in an extensive literature review; 66 unique data points from 19 different studies. There is one nonunique data point in Table 1 from two papers by Foote and Andrew,[52,53] included here to

avoid future confusion. Foote and Andrew reported the same data point in two different studies in 1905,[52,53] and those data points should not be taken as two separate unique measurements. Two additional studies reported their data only graphically, and those data were not included in Table 1.[61,62]

Table 1 reports the data in the units reported by the original authors but also converts the data to molality (moles per kilogram of water; mol/kg). In two studies, the data were originally reported in molarity units, but no density or water content of the saturated solution is available to convert to mol/kg.[48,56] For those studies, the water contents were estimated using the Laliberte-Cooper model,[63] using the method of Reynolds and Carter[64] and the coefficients from the electronic appendix of Lalibete.[65] Lalibete developed those coefficients based on the data from references,[66,67] which were measured below saturation. Consequently, the Laliberte-Cooper model was slightly extrapolated to concentrations higher than those in the measured data. The data converted with the Laliberte-Cooper model are reported in Table 1 but were not used in the computational analysis below. The value calculated at 298.15 K for the Britton and Jarrett[48] data point was exactly on the mean solubility for this temperature discussed in the next section.

The value calculated for the Matyukha et al.[56] data point was somewhat higher than the mean at 0.281 mol/kg.

The solubility of disodium oxalate is an approximately linear function of temperature (Figure 1). Most data were clustered
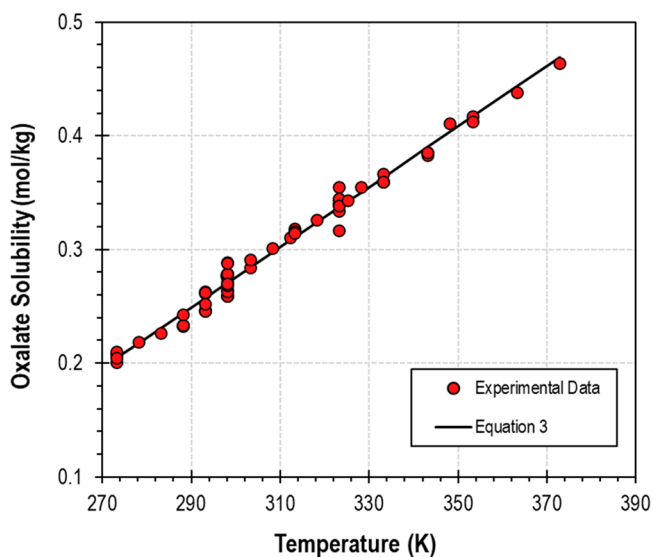

Figure 1. Plot of disodium oxalate solubility as a function of the temperature between 273 and 373 K.

near the line. At 298.15 K, the solubility measurements range between 0.259 and 0.289 mol/kg. At 323.15 K, the solubility measurements range between 0.317 and 0.355 mol/kg. However, if the highest and lowest concentrations at 323.15 K are removed, the range narrows to between 0.33 and 0.34 mol/kg.

■ COMPUTATIONAL ANALYSIS

A line was fit to the data in Table 1 using the linear regression function in a Microsoft Excel 365 spreadsheet. Equation 3 is the regression equation, where T is temperature in kelvin, while a and b are empirically determined parameters:

$$\text{Disodium oxalate solubility, mol/kg} = aT + b \qquad (3)$$

The line is shown in Figure 1, and the regression statistics and parameters are shown in Table 2. The high coefficient of

Table 2. Parameters for eq 3 and Regression Statistics

parameter or statistic	all data	all data minus refs 44 and 45
a	$0.002655 \pm 4.3 \times 10^{-05}$	$0.002716 \pm 7.2 \times 10^{-05}$
b	-0.52101 ± 0.001	-0.54044 ± 0.02
standard error	0.00782	0.009132
R^2	0.984	0.973

determination R^2 (0.984) and the good fit shown graphically in Figure 1 support the conclusion that the data are approximately linear over this temperature range. The slope of the line indicates that the solubility of disodium oxalate increases by approximately 0.0027 mol/kg per K increase. Two studies had many data points at different temperatures. Norris reported measurements at ten temperatures between 273 and 372.78 K.[45] Menczel et al. reported data at 12 temperatures between 273.15 and 328.15 K.[44] Together, these two studies account for one-third of the data in Table 1. To be sure the

linear trend is not the result of bias from these two studies, eq 3 was also fit to all of the data excluding these two studies. The regression statistics are listed in Table 2.

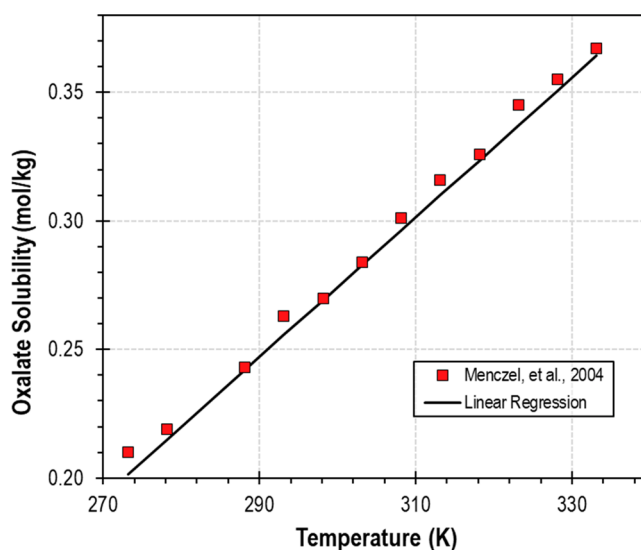Figure 2 compares all the data minus Norris and Menczel equation to the data from Menczel et al.,[44] which are data not

Figure 2. Comparison of the regression equation called "All Data Minus Norris and Menczel" with data from Menczel et al.[44]

used to develop this equation. There is a small bias in these data, with the data on average being slightly higher than the regression equation. Nonetheless, the agreement between the linear model and the data is close.

Figure 3 compares the All Data Minus Norris and Menczel equation to the data from Norris,[45] which is data not used to
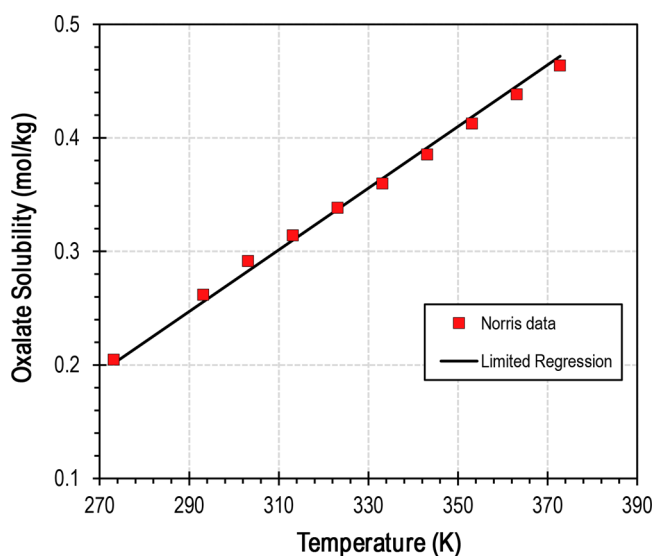

Figure 3. Comparison of the regression equation called "All Data Minus Norris and Menczel" with data from Norris.[45]

develop this equation. Norris[45] reports ten data points between 273 and 373 K. The prediction of the Norris data is excellent. Note that Norris[45] provides the only two data points above 353 K. The regressing equation provides an excellent prediction of Norris' data points at 363 and 373 K even

Table 3. Parameters for eq 5 for the Solids and Ions Used in This Study

constituent	A	B	C	D	E	ref
Na+	−105.73	0.85194	0	0	−0.000883	69
$C_2O_4^{-2}$	−272.165	2.782581	0	0	−0.002792	68
$Na_2C_2O_4$	−489.4015	5.041464	37072.55	−247.939	−0.004768	29

though no data above 353 K was used to parametrize the equation. These results indicate that large data sets from Menczel et al.[44] as well as Norris[45] are consistent with the other data in the data sets.

Of note is that both regression equations in Table 2 had identical slopes. This shows that the two large data sets did not bias the regression, and supports the conclusion that the solubility of disodium oxalate increases 0.0027 mol/kg/K.

There is more data at 298.15 K than any other temperature. The mean concentration of all of the measurements at 298.15 K is 0.274 mol/kg. The standard error for the solubility data at 298.15 K is 0.0026 mol/kg. When eq 1 is solved at 298.15 K using the coefficients fit to all data, the disodium oxalate solubility is 0.272 mol/kg, within the standard error of the mean value.

In a previous study,[29] the authors developed a model for the solubility of disodium oxalate in water based solely on the data in reference.[45] Here it is tested against all of the data in Table 1. The Pitzer equations (eqs 1 and 2) were used to calculate the solution phase activity coefficients, taken from ref 68. In order to be consistent with the large number of thermodynamic parameters from the references,[68,69] the Gibbs free energies at standard state ($\mu°$) are calculated as reduced chemical potentials (μ) per eq 4.

$$\mu_j = \frac{\mu^o}{RT} \tag{4}$$

Here, R is the Universal Gas Constant. The μ_j values are empirical functions of temperature (eq 5) where A, B, C, D, and E are parameters shown in Table 3:

$$\mu_j \text{ at } T = A + B(T - T_r) + C\left(\frac{1}{T_r} - \frac{1}{T}\right) + D\ln\left(\frac{T}{T_r}\right)$$
$$+ E(T^2 - T_r^2) \tag{5}$$

The solubility of disodium oxalate was calculated using eqs 1, 2, 4, and 5 as described in ref 29 with the comparison to the data in Table 1 shown in Figure 4. These results indicate that there is reasonable agreement with the model with the data.

■ DISCUSSION

Solid disodium oxalate is monoclinic with a $P2/c$ space group.[70,71] In Hanford waste, disodium oxalate displays a thin needle morphology between 10 and 200 μm long.[19] Many other morphologies can be precipitated from aqueous solutions in the presence of other ions.[72] The oxalate ion forms a planar structure (D_{2h} space group) in solid disodium oxalate. Oxalate is rotated into a D_{2d} space group in aqueous solution because of hydrogen bonding between water and oxalate.[73]

Dissolved oxalate forms weak ion-pairs with Na$^+$, ion pairing that likely influences the solubility of disodium oxalate.[74−76] The strength of ion-pairing decreases with increasing ionic strength.[75] The reaction for the ion-pair is written:

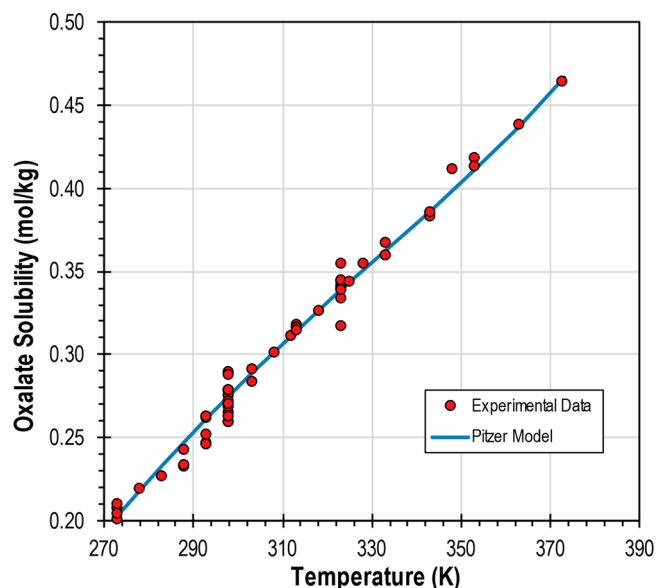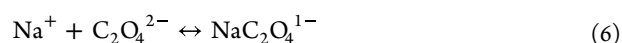$$Na^+ + C_2O_4^{2-} \leftrightarrow NaC_2O_4^{1-} \tag{6}$$

Figure 4. Comparison of experimental data to thermodynamic model from ref 29.

In dilute solutions, there are two water molecules in between the Na$^+$ and oxalate ions in the ion pair, called a two-solvent shared ion-pair.[76]

With a formal charge of negative two, oxalate has a −0.5 charge per oxygen. Assuming that each oxalate oxygen is coordinated by three cations on average, oxalate has an average bond valence of −0.17 per coordinating cation.[77] Gagné and Hawthorne determined that Na$^+$ has an average bond valence of 0.16, averaged over many crystal structures.[78] Brown indicates that stable structures are formed when the cation and anion have nearly matching opposite bond valence,[79] as is the case here with Na$^+$ and oxalate. Stable solids would expect to have a low solubility in water and other solvents. The low solubility of disodium oxalate may thus be because of the excellent matching bond valence of the ions. What constitutes "low solubility" is subjective, so it is quantified here by comparing the solubility of disodium oxalate to that of other alkali oxalates at 298 K. A recent study on monovalent cation nitrates shows that the monovalent cations that most closely matched nitrate's bond valence had the lowest solubilities.[80]

While an in-depth evaluation of the solubility of other alkali oxalates was not undertaken, Foote and Andrew reported the solubility of lithium, potassium, and cesium oxalate at 298 K.[52] Their measured concentration of disodium oxalate at 298.15 K (0.279 mol/kg) agrees well with the mean concentration of 0.274 mol/kg determined here, suggesting that their measurement of the solubility of other alkali oxalates was likely reasonably accurate as well. Figure 5 plots the solubility of disodium oxalate along with the solubility of other alkali oxalates reported by Foote and Andrew against the bond valence values for the alkali ions from Gagné and Hawthorne.[52,78] The bond valence of sodium most closely matches the bond valence of the oxalate oxygens, and it also
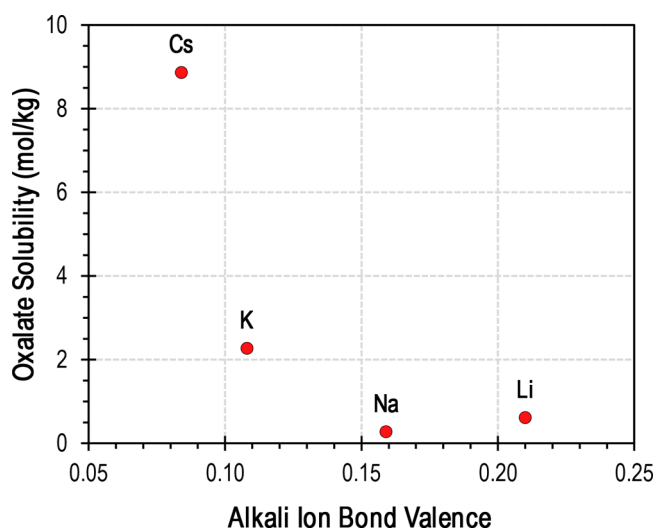
Figure 5. Alkali oxalate solubility in water vs alkali bond valence. The disodium oxalate solubility value is the mean value from this study, the rest of the solubility data are from Foote and Andrew.[52]

has the lowest solubility (Figure 5). Lithium has the next closest average bond valence of 0.21, and it has the next closest solubility in water to that of disodium oxalate. Potassium and cesium have bond valences much further from oxalate's than sodium and lithium and exhibit much larger solubilities (Figure 5). This is consistent with Brown's theory[79] that structures with matching bond valences of the counterions will be the most stable, here demonstrated using solubility data.

Sodium and lithium have the closest matching opposite bond valence to oxalate, and they both crystallize as anhydrous salts.[70,71,81] Potassium and cesium have bond valences that match poorly with oxalate, and both crystallize as hydrated salts at 298 K with water partially separating the cation from the oxalate.[82−84] Hawthorne and Schindler[85] indicate that salts incorporate water into their crystal structure to moderate bond valence differences between cation and anion, which was verified for many oxalates by Echigo and Kimata.[77] The two hydrated salts in Figure 5 also had the highest solubility, consistent with the relative instability of these alkali oxalates. The anhydrous forms of cesium and potassium oxalates would presumably be even more soluble in water, a hypothesis that may not be testable because they have only been synthesized when water is excluded.[86]

The Hanford Site currently plans to vitrify radioactive waste solids into high-level waste glass.[87] The Site plans to dissolve nonradioactive soluble salts from the solids to minimize the mass vitrified as high-level waste.[88] Disodium oxalate is one of the least soluble salts in the waste. As mentioned in the Introduction, the Hanford Site has about 16 million moles of oxalate in its radioactive waste storage tanks. It would require 58 million kilograms of water to dissolve this oxalate at 298 K. Oxalate is readily destroyed in the melter if vitrified, but the accompanying sodium decreases the durability of the glass produced.[89,90] Nonetheless, some sodium is needed to condition the molten glass viscosity and electrical conductivity.[91,92] Consequently, the amount of sodium sent to the melter must be balanced for optimal treatment.[87] The solubility of disodium oxalate is thus an important input to waste treatment flowsheets at Hanford.

CONCLUSIONS

The solubility data of disodium oxalate measured across 19 studies was highly consistent with each other. A regression analysis of the data determined that nearly identical results were obtained when a linear model was fit to the data with or without two large data sets accounting for 1/3 of the data. This indicates that these two large data sets and all the rest of the data are consistent with each other. The mean solubility measurement at 298.15 K was 0.274 mol/kg, and there was a tight standard error around the mean of only 0.0026 mol/kg, indicating that the true solubility at 298.15 K is likely very near this mean value. When the regression equation was solved at 298.15 K, a solubility of 0.272 mol/kg was determined, which was also supportive of the mean solubility at 298.15 being approximately equal to the real solubility.

The solubility of disodium oxalate increased by approximately 0.0027 mol/kg/K, with an error of only 4.3×10^{-05} mol/kg/K, indicating that there is high confidence in this temperature dependence.

The solubility of disodium oxalate is low because of the closely matching opposite bond valences of Na^+ and oxalate. This was shown by comparing the solubility of disodium oxalate to other alkali oxalates, where disodium oxalate had the lowest solubility and the most closely matching opposite bond valence to oxalate. Matching bond valence analysis has been used for many years to determine the stability of different crystal structures. Here, it shown that matching bond valences can be used to explain relative solubilities of different oxalate salts.

AUTHOR INFORMATION

Corresponding Author

    Jacob G. Reynolds − *Washington River Protection Solutions, LLC, Richland, Washington 99352, United States;* orcid.org/0000-0001-6091-8540;
    Email: jacob_g_reynolds@rl.gov

Authors

    Michael D. Britton − *Washington River Protection Solutions, LLC, Richland, Washington 99352, United States*
    Robert Carter − *Washington River Protection Solutions, LLC, Richland, Washington 99352, United States*

Complete contact information is available at:
https://pubs.acs.org/10.1021/acs.iecr.3c01362

Notes

The authors declare no competing financial interest.

REFERENCES

(1) Akatsu, J. Separation of Pu-Am from an Aqueous Waste by Successive Oxalate and Lead Oxalate Precipitations. *Sep. Sci. Technol.* **1982**, *17*, 1433−1442.

(2) Rao, V. K.; Pius, I. C.; Subbarao, M.; Chinnusamy, A.; Natarajan, P. R. Precipitation of Plutonium Oxalate from Homogeneous Solutions. *J. Radional. Nucl. Chem.* **1986**, *100*, 129−134.

(3) Zhang, Z.; Jia, Q.; Liao, W. Progress in the Separation Processes for Rare Earth Resources. *Handbook on the Physics and Chemistry of Rare Earths* **2015**, *48*, 287−376.

(4) Prodius, D.; Klocke, M.; Smetana, V.; Alammar, T.; Perez Garcia, M.; Windus, T. L.; Nlebedim, I. C.; Mudring, A.-V. Rationally Designed Rare Earth Separation by Selective Oxalate Solubilization. *Chem. Commun.* **2020**, *56*, 11386−11389.

(5) Chen, Z.; Li, Z.; Chen, J.; Kallem, P.; Banat, F.; Qiu, H. Recent Advances in Selective Separation Technologies of Rare Earth Elements: A Review. *J. Environ. Chem. Eng.* **2022**, *10*, 107104.

(6) Forsberg, C. W. Separation of Americium, Curium, and Trivalent Lanthanides from High-Level Wastes by Oxalate Precipitation: Experiments with Synthetic Waste Solutions. *Nucl. Technol.* **1980**, *49*, 243−252.

(7) Hofmann, B. A.; Bernasconi, S. M. Review of Occurrences and Carbon Isotope Geochemistry of Oxalate Minerals: Implications for the Origin and Fate of Oxalate in Diagenetic and Hydrothermal Fluids. *Chem. Geol.* **1998**, *149*, 127−146.

(8) Echigo, T.; Kimata, M. Crystal Chemistry and Genesis of Organic Minerals: A Review of Oxalate and Polycyclic Aromatic Hydrocarbon Minerals. *Can. Min.* **2010**, *48*, 1329−1357.

(9) Khafhafera, A. N.; Kung, J. W. J.; DeMartini, N. Solubility of Sodium Oxalate in Kraft Black Liquors below 100°C. *Can. J. Chem. Eng.* **2023**, *101*, 819−827.

(10) Li, H.; Chai, X. S.; DeMartini, N. Oxalate Release and Formation during Alkaline Pulping. *J. Wood Chem. Technol.* **2012**, *32*, 187−197.

(11) Machold, T.; Macedi, E.; Laird, D. W.; May, P. M.; Hefter, G. T. Decomposition of Bayer Process Organics: Low-Molecular-Weight Carboxylates. *Hydromet.* **2009**, *99*, 51−57.

(12) Moreno, R. A.; Falconi, I. B. A.; Gonçalves, T. A. M.; Seno Junior, R.; Espinosa, D. C. R.; Tenório, J. A. S. Sodium Recovery from Crystallization Waste of Bayer Liquor in Alumina Beneficiation. *Can. J. Chem. Eng.* **2022**, *100*, S225−S235.

(13) Ulmgren, P.; Rådeström, R. Deposition of Sodium Oxalate in the Black Liquor Evaporation Plant. *Nordic Pulp Paper Res. J.* **2002**, *17*, 275−279.

(14) Verma, A.; Corbin, D. R.; Shiflett, M. B. Extraction of Aluminum and Iron from Bauxite: A Unique Closed Loop Ore Refining Process Utilizing Oxalate Chemistry. *AIChE J.* **2022**, *68*, e17477.

(15) Verma, A.; Henne, A. J.; Corbin, D. R.; Shiflett, M. B. Lithium and Cobalt Recovery from $LiCoO_2$ Using Oxalate Chemistry: Scale-Up and Techno-Economic Analysis. *Ind. Eng. Chem. Res.* **2022**, *61*, 5285−5294.

(16) Warrant, R. W.; Cooke, G. A. Characterization of the Solids Waste in the Hanford Waste Tanks Using a Combination of XRD, SEM and PLM. *Adv. X-Ray Anal.* **2003**, *46*, 251.

(17) Sharma, A. K.; Clauss, S. A.; Mong, G. M.; Wahl, K. L.; Campbell, J. A. Analysis and Quantification of Organic Acids in Simulated Hanford Tank Waste and Hanford Tank Waste. *J. Chrom. A* **1998**, *805*, 101−107.

(18) Reynolds, J. G.; Cooke, G. A.; Herting, D. L.; Warrant, R. W. Evidence for Dawsonite in Hanford High-Level Nuclear Waste Tanks. *J. Hazard. Mater.* **2012**, *209–210*, 186.

(19) Reynolds, J. G.; Cooke, G. A.; Herting, D. L.; Warrant, R. W. Salt Mineralogy of Hanford High-Level Nuclear Waste Staged for Treatment. *Ind. Eng. Chem. Res.* **2013**, *52* (29), 9741−9751.

(20) Meznarich, H.; Penchoff, D. A. A Brief on Nuclear Waste at the Hanford Site and a Computational Analysis of Uranyl Nitrate with and without Tributyl Phosphate. *Rare Earth Elements and Actinides: Progress in Computational Science Applications* **2021**, *1388*, 101.

(21) Toste, A. P.; Lechner-Fish, T. J.; Scheele, R. D. Organics in a Hanford Mixed Waste Revisited: Myriad Organics and Chelator Fragments Unmasked. *J. Radioanal. Nucl. Chem.* **2013**, *296*, 523−530.

(22) Toste, A. P. Degradation of Chelating and Complexing Agents in an Irradiated, Simulated Mixed Waste. *J. Radioanlyt. Nucl. Chem.* **1992**, *161*, 549−559.

(23) Toste, A. P. Gamma Radiolysis of EDTA in a Simulated, mixed Nuclear Waste. *J. Radioanal. Nucl. Chem.* **1998**, *235*, 213−219.

(24) Toste, A. P. Detailed Study of the γ-Radiolysis of Nitrilotriacetatic acid in a Simulated, Mixed Nuclear Waste. *J. Radioanal. Nucl. Chem.* **1999**, *239*, 433−439.

(25) Toste, A. P.; Pilot, T. Detailed Study of HEDTA's Chemodynamics upon Gamma-Radiolysis in a Simulated, Mixed Waste. *J. Radionalytical Nucl. Chem.* **2008**, *277*, 5−10.

(26) Poirier, M. R.; Hay, M. S.; Herman, D. T.; Crapse, K. P.; Thaxton, G. D.; Fink, S. D. Removal of Sludge Heels in Savannah River Site Waste Tanks with Oxalic Acid. *Sep. Sci. Technol.* **2010**, *45*, 1858−1875.

(27) Deutsch, W. J.; Cantrell, K. J.; Krupka, K. M.; Lindberg, M. L.; Serne, R. J. Hanford Tank Residual Waste - Contaminant Source Terms and Release Models. *Appl. Geochem.* **2011**, *26*, 1681−1693.

(28) Russell, R. L.; Snow, L. A.; Peterson, R. A. Methods to Avoid Post-Filtration Precipitation in Treatment of High-Level Waste. *Sep. Sci. Technol.* **2010**, *45*, 1814−1821.

(29) Carter, R.; Pierson, K. L.; Reynolds, J. G., Binary Pitzer Model Parameters for Predicating the Solubility of Key Electrolytes in Hanford Waste. Proceedings of Waste Management 2014; Waste Management Symposia Inc., Tucson, AZ, March 2-6, *Proceedings of Waste Management 2014* 2014.

(30) Reynolds, J. G.; Carter, R. Pitzer Model Anion-Anion and Ternary Interaction Parameters for the $Na_2C_2O_4$-$NaOH$-H_2O and $Na_2C_2O_4$-$NaNO_3$-H_2O Systems. *J. Sol. Chem.* **2015**, *44*, 1358−1366.

(31) Reynolds, J. G. Application of Mixture Models to Solubility Calculations, Using Sodium Oxalate as an Example. *Sep. Sci. Technol.* **2008**, *43*, 2872−2886.

(32) Qafoku, O.; Felmy, A. R. Development of Accurate Chemical Equilibrium Models for Oxalate Species to High Ionic Strength in the System: Na-Ba-Ca-Mn-Sr-Cl-NO_3-PO_4-SO_4-H_2O at 25 °C. *J. Sol. Chem.* **2007**, *36*, 81−95.

(33) Dean, J. A. *Lange's Handbook of Chemistry*; 13th ed.; McGraw Hill, Inc.: New York, NY, 1985.

(34) Dean, J. A. *Lange's Handbook of Chemistry*. 15th ed.; McGraw Hill, Inc.: New York, NY, 1999.

(35) Partanen, J. I.; Juusola, P. M.; Covington, A. K. Re-Evaluation of the First and Second Stoichiometric Dissociation Constants of Oxalic Acid at Temperatures from 0 to 60 °C in Aqueous Oxalate Buffer Solutions With or Without Sodium or Potassium Chloride. *J. Sol. Chem.* **2009**, *38*, 1385−1416.

(36) Eysseltova, J.; Zbranek, V.; Skripkin, M. Y.; Sawada, K.; Tepavitcharova, S. IUPAC-NIST Solubility Data Series. 89. Alkali Metal Nitrates. Part 2. Sodium Nitrate. *J. Phys. Chem. Ref. Data* **2017**, *46*, 013103.

(37) Krumgalz, B. S. Temperature Dependence of Mineral Solubility in Water. Part 3. Alkaline and Alkaline Earth Sulfates. *J. Phys. Chem. Ref. Data* **2018**, *47*, 023101.

(38) Reynolds, J. G.; Britton, M. D.; Belsher, J. D. A Review of Sodium Nitrite Solubility in Water and Physical Properties of the Saturated Solutions. *J. Chem. Eng. Data* **2021**, *66*, 2931−2941.

(39) Reynolds, J. G.; Belsher, J. D. A Review of Sodium Fluoride Solubility in Water. *J. Chem. Eng. Data* **2017**, *62*, 1743−1748.

(40) Reynolds, J. G. Salt Solubilities in Aqueous Solutions of $NaNO_3$, $NaNO_2$, $NaCl$, and $NaOH$: A Hofmeister-like Series for Understanding Alkaline Nuclear Waste. *ACS Omega* **2018**, *3*, 15149−15157.

(41) Pitzer, K. S. Ed. Ion interaction approach: theory and data correlation. In *Activity Coefficients in Electrolyte Solutions*, 2nd ed.; CRC Press: Boca Raton, FL, 1991; pp 75−153.

(42) Foote, H. W.; Vance, J. E. The System: Sodium Iodate, Sodium Oxalate, Water. *Am. J. Sci.* **1933**, *151*, 16−18.

(43) Hill, L. M.; Goulden, T. P.; Hatton. Equilibria in Ternary Systems Containing Oxalates. *J. Chem. Soc.* **1946**, 78−81.

(44) Menczel, B.; Apelblat, A.; Korin, E. The Molar Enthalpies of Solution and Solubilities of Ammonium, Sodium and Potassium Oxalates in Water. *J. Chem. Thermo.* **2004**, *36*, 41−44.

(45) Norris, W. H. H. The System Oxalic Acid-Sodium Hydroxide-Water. *J. Chem. Soc.* **1951**, *0*, 1708−1715.

(46) Zhao, H. K.; Zhang, D. S.; Tang, C.; Li, R. R.; Su, M. L.; Xu, W. L.; Wang, Y. Q. Solubility and Phase Diagram for the Ternary Sodium Oxalate + Hydrogen Peroxide + Water System at (283.15 and 293.15) K. *J. Chem. Eng. Data* **2007**, *52*, 863−865.

(47) Flöttmann, F. Über Löslichkeitsgleichwichte. *Fresenius, Zeitschrift f. Anal. Chem.* **1928**, *73*, 1−39.

(48) Britton, H. T. S.; Jarrett, M. E. D. Physichochemical Studies of Complex Formation Involving Weak Acids. Part XVI. (a) Isotherms at 18° of the Systems: Sodium Oxalate-Copper (or Zinc or Magnesium) Oxalate-Water. (b) The Solubility of Copper, Zinc, and Magnesium Oxalates in Solutions of Oxalic acid and Sulphuric Acid. (c) Potentiometric Investigation of the Complex Anion, $Cu(C_2O_4)_2$. *J. Chem. Soc.* **1936**, *0*, 1489−1493.

(49) Zhikharev, M. I.; Kol'ba, V. I.; Sukhanov, L. P. The $Na_2C_2O_4$-$NaNO_3$-H_2O System at 20 °C. *Russ. J. Inorg. Chem.* **1979**, *24*, 46.

(50) Elod, E.; Acker, E. Das Quaternare System $Na_2C_2O_4$-H_2SO_4-Na_2SO_4 (bzw. $H_2C_2O_4$)-H_2O bei 25 °C). *Z. Anorg. Allg. Chem.* **1928**, *176*, 305−324.

(51) Britton, H. T. S.; Jarrett, M. E. D. Physichochemical Studies of Complex Formation Involving Weak Acids. Part XVII. The System Sodium Oxalate-Thorium Oxalate-Water at 25°. *J. Chem. Soc.* **1936**, *0*, 1494−1497.

(52) Foote, H. W.; Andrew, I. A. The Acid Oxalates of Lithium, Sodium, Potassium and Caesium and Their Solubility. *American Chemical Journal* **1905**, *34*, 153−164.

(53) Foote, H. W.; Andrew, I. A. On Certain Alleged Double Oxalates. *American Chemical Journal* **1905**, *34*, 164−167.

(54) Hefter, G.; Tromans, A.; May, P. M.; Königsberger, E. Solubility of Sodium Oxalate in Concentrated Electrolyte Solutions. *J. Chem. Eng. Data* **2018**, *63*, 542−552.

(55) Kovaleva, I. S.; Luzhnaya, N. P. Solubility Isotherm of the $Th(C_2O_4)_2 + 2Na_2CO_3 \leftrightarrow Th(CO_3)_2 + 2Na_2C_2O_4$ - H_2O Quaternary Reciprocal System at 25 °C. *Russ. J. Inorg. Chem.* **1962**, *7*, 873−875.

(56) Matyokha, V. A.; Krot, N. N.; Gel'man, A. D. The Form in Which Plutonium(IV) Exists in Oxalate Solutions. *Russ. J. Inorg. Chem.* **1968**, *13*, 1099−1102.

(57) Rivett, A. C. D.; O'Connor, E. A. CXXV.—Some Ternary Systems Containing Alkali Oxalates and Water. *J. Chem. Soc., Trans.* **1919**, *115*, 1346−1354.

(58) Boulanger, J. Suite de L'étude de Systems Oxalate de Zirconyle, Oxalates Alcalines et eau, [Translation: "Continuation of the Study of Zirconyl Oxalate Systems, Alkaline Oxalates and Water"]. *Compt. Rend.* **1936**, *203*, 87−90.

(59) Colani, M. A.; Haller, M. A. Etude du Systeme Eau Oxalate d'Uranyl, Oxalate de Sodium. *Comptes Rendus Hebdomadaires De L'academia Des Sci.* **1917**, 111−113.

(60) Kol'ba, V. I.; Zhikharev, M. I.; Sukhanov, L. P. The $Na_2C_2O_4$-$NaNO_3$-H_2O System at 50° and 75 °C. *Russ. J. Inorg. Chem.* **1980**, *25*, 1583−1584.

(61) Buttke, L. G.; Schueller, J. R.; Pearson, C. S.; Beyer, K. D. Solubility of the Sodium and Ammonium Salts of Oxalic Acid in Water with Ammonium Sulfate. *J. Phys. Chem. A* **2016**, *120*, 6424−6433.

(62) Rozaini, M. Z. H.; Brimblecombe, P. The Solubility Measurements of Sodium Dicarboxylate Salts; Sodium Oxalate, Malonate, Succinate, Glutarate, and Adipate in Water from T = (279.15 to 358.15) K. *J. Chem. Thermo.* **2009**, *41*, 980−983.

(63) Laliberte, M.; Cooper, W. E. Model for Calculating the Density of Aqueous Electrolyte Solutions. *J. Chem. Eng. Data* **2004**, *49*, 1141−1151.

(64) Reynolds, J. G.; Carter, R. Reconciliation of Solute Concentration Data with Water Contents and Densities of Multi-Component Electrolyte Solutions. *J. Sol. Chem.* **2008**, *37*, 1113−1125.

(65) Laliberte, M. A Model for Calculating the Heat Capacity of Aqueous Solutions, with Updated Density and Viscosity Data. *J. Chem. Eng. Data* **2009**, *54*, 1725−1760.

(66) Taft, R.; Welch, F. H. Physical Properties of Aqueous Solutions of Sodium Oxalate, Sodium Malonate, and Sodium Succinate, I. *Tr. Kansas Acad. Sci.* **1951**, *54*, 233−246.

(67) Tromans, A.; Königsberger, E.; May, P. M.; Hefter, G. Heat Capacities and Volumes of Aqueous Dicarboxylate Salt Solutions of Relevance to the Bayer Process. *J. Chem. Eng. Data* **2005**, *50*, 2019−2025.

(68) Steele, W. F.; Weber, C. F.; Bostick, D. A. *Waste and Simulant Precipitations Issues, ORNL/TM-2000/348;*Oak Ridge National Laboratory:Oak Ridge, TN, 2000.

(69) Weber, C. F.; Beahm, E. C.; Lee, D. D.; Watson, J. S. A Solubility Model for Aqueous Solutions Containing Sodium, Fluoride, and Phosphate Ions. *Ind. Eng. Chem. Res.* **2000**, *39*, 518−526.

(70) Jeffrey, G. T.; Parry, G. S. The Crystal Structure of Sodium Oxalate. *J. Am. Chem. Soc.* **1954**, *76*, 5283−5286.

(71) Reed, D. A.; Olmstead, M. M. Sodium Oxalate Structure Refinement. *Acta Crystallogr.* **1981**, *B37*, 938−939.

(72) Fu, W.; Vaughan, J.; Gillespie, A. Effects of Inorganic Anions on the Morphology of Sodium Oxalate Crystallized from Highly Alkaline Solutions. *Cryst. Growth Des.* **2014**, *14*, 1972−1980.

(73) Hind, A. R.; Bhargava, S. K.; Van Bronswijk, W.; Grocott, S. C.; Eyer, S. L. On the Aqueous Vibrational Spectra of Alkali Metal Oxalates. *Appl. Spectrosc.* **1998**, *52*, 683−691.

(74) Singh, R. P. On the Existence of the $NaC_2O_4^-$ Ion Pair Complex. *Bull. Chem. Soc. Jpn.* **1989**, *62*, 4089−4091.

(75) Tromans, A.; Hefter, G.; May, P. M. Potentiometric Investigation of the Weak Association of Sodium and Oxalate Ions in Aqueous Solutions at 25 °C. *Aust. J. Chem.* **2005**, *58*, 213−217.

(76) Buchner, R.; Samani, F.; May, P. M.; Sturn, P.; Hefter, G. Hydration and Ion Pairing in Aqueous Sodium Oxalate Solutions. *ChemPhysChem* **2003**, *4*, 373−378.

(77) Echigo, T.; Kimata, M. The Common Role of Water Molecule and Lone Electron Pair as a Bond-Valence Mediator in Oxalate Complexes: The Crystal Structures of $Rb_2(C_2O_4) \cdot H_2O$ and $Tl_2(C_2O_4)$. *Z. Kristallogr.* **2006**, *221*, 762−769.

(78) Gagné, O. C.; Hawthorne, F. C. Empirical Lewis Acid Strengths for 135 Cations Bonded to Oxygen. *Acta Crystallogr.* **2017**, *B73*, 956−961.

(79) Brown, I. D. Recent Developments in the Methods and Applications of the Bond Valence Model. *Chem. Rev.* **2009**, *109*, 6858−6919.

(80) Reynolds, J. G. Solubilities in Aqueous Nitrate Solutions that Reverse the Law of Mass Action. *Phys. Chem. Chem. Phys.* **2021**, *23*, 21407−21418.

(81) Beagley, B.; Small, R. W. H. The Structure of Lithium Oxalate. *Acta Crystallogr.* **1964**, *17*, 783−788.

(82) Hodgson, D. J.; Ibers, J. A. Refinement of the Crystal and Molecular Structure of Potassium Oxalate Monohydrate. *Acta Cryst. B* **1969**, *25*, 469−477.

(83) Kholodkovskaya, L. N.; Trunov, V. K.; Tskhelashvili, N. B. Crystal Structures of Cesium Hydrogenoxalate and Cesium Oxalate Dihydrate. *J. Struct. Chem.* **1991**, *31*, 667−670.

(84) McGrath, J. W.; Paine, A. A. Motion of the H_2O Molecule in Potassium Oxalate Monohydrate. *J. Chem. Phys.* **1964**, *41*, 3551−3555.

(85) Hawthorne, F. C.; Schindler, M. Understanding the Weakly Bonded Constituents in Oxysalt Minerals. *Z. Kristallogr.* **2008**, *223*, 41−68.

(86) Dinnebier, R. E.; Vensky, S.; Panthöfer, M.; Jansen, M. Crystal and Molecular Structures of Alkali Oxalates: First Proof of a Staggered Oxalate Anion in the Solid State. *Inorg. Chem.* **2003**, *42*, 1499−1507.

(87) Goel, A.; McCloy, J. S.; Pokorny, R.; Kruger, A. A. Challenges with Vitrification of Hanford High-Level Waste (HLW) to Borosilicate Glass - An Overview. *J. Non-Cryst. Solids X* **2019**, *4*, 100033.

(88) McGinnis, C. P.; Welch, T. D.; Hunt, R. D. Caustic Leaching of High-Level Radioactive Tank Sludge: A Critical Literature Review. *Sep. Sci. Technol.* **1999**, *34*, 1479.

(89) Hujova, M.; Pokorny, R.; Klouzek, J.; Lee, S.; Traverso, J. J.; Schweiger, M. J.; Kruger, A. A.; Hrma, P. Foaming During Nuclear Waste Melter Feeds Conversion to Glass: Application of Evolved Gas Analysis. *Int. J. Appl. Glass Sci.* **2018**, *9*, 487−498.

(90) Vienna, J. D.; Crum, J. V. Non-Linear Effects of Alumina Concentration on Product Consistency Test Response of Waste Glasses. *J. Nucl. Mater.* **2018**, *511*, 396−405.

(91) Hrma, P.; Kruger, A. A. High-Temperature Viscosity of Many-Component Glass Melts. *J. Non-Cryst. Solids* **2016**, *437*, 17−25.

(92) Vienna, J. D.; Hrma, P.; Kim, D. S.; Schweiger, M. J.; Smith, D. E. Compositional Dependence of Viscosity, Electrical Conductivity, and Liquidus Temperature of Multicomponent Borosilicate Waste Glasses. *Ceram. Trans.* **1996**, *72*, 427−436.